11.9 W Output Power at S-band from 1 mm AlGaN/GaN HEMTs

M.C.J.C.M. Krämer[a], F. Karouta[a], J.J.M. Kwaspen[a], M. Rudzinski[b], P.K. Larsen[b], E.M. Suiker[c], P.A. de Hek[c], T. Rödle[d], Iouri Volokhine[e] and L.M.F. Kaufmann[a]

[a]COBRA Inter-University Research Institute on Communication Technology,
Eindhoven University of Technology, P.O. Box 513, 5600 MB Eindhoven,
The Netherlands
[b]Applied Materials Science Institute for Molecules and Materials, Radboud University,
6500 GL Nijmegen, The Netherlands
[c]TNO Defence, Security and Safety, P.O. Box 96864, 2509 JG The Hague,
The Netherlands
[d]NXP Semiconductors, Gerstweg 2, P.O. Box 30008, 6503 HK Nijmegen,
The Netherlands
[e]NXP Semiconductors, Research, High Tech Campus, Prof. Holstlaan 4, 5656 AA
Eindhoven, The Netherlands

We present radio-frequency (RF) power results of GaN-based high electron mobility transistors (HEMTs) with total gate widths (W_g) up to 1 mm. The AlGaN/GaN epi-structures are MOVPE-grown on 2-inches semi-insulating (s.i.) 4H-silicon carbide substrates. The HEMTs have been fabricated using an optimized process flow comprising a low-power Ar-based plasma after ohmic contact metallization, cleaning of the AlGaN surface prior to the Schottky gate metallization using a diluted ammonia (NH_4OH) solution, and passivation of the AlGaN surface using a silicon nitride layer deposited by plasma enhanced chemical vapor deposition.
We will show that the best RF power performance has been achieved by HEMTs with iron-doped GaN buffer layers (GaN:Fe). Devices with a total gate width of 1 mm yielded a maximum output power of 11.9 W at S-band (2 - 4 GHz) under class AB bias conditions (V_{DS} = 40 - 60 V, and V_{GS} = -4.65 – - 4.0 V).

Introduction

GaN-based high electron mobility transistors (HEMTs) are very attractive for high-power high-frequency electronics because of the high electric breakdown field and the high saturation velocity of electrons. The maximum drain current densities of AlGaN/GaN HEMTs range from 1.0 - 1.5 A/mm [1-3]. Hence, it is obvious that breakdown voltages over 160 V are required to achieve record output power densities larger than 30 W/mm [3] for class A operation. Generally, GaN-based HEMTs yield maximum radio-frequency (RF) output powers that are significantly less than the values that can be estimated from their direct-current (DC) characteristics. The responsible current collapse mechanism, which is generally indicated as DC-to-RF current-dispersion or gate lag, is caused by traps located at the AlGaN surface that capture the electrons from the two-dimensional electrons gas (2DEG), which is present at the AlGaN/GaN heterojunction [4]. From [4] it is also known that passivation of the surface of the AlGaN barrier layer with high-quality plasma enhanced chemical vapour deposition (PECVD) silicon nitride (SiN_x) significantly reduces this current dispersion effect. However, after this passivation a significant increase in the gate and drain leakage current densities may be observed. Although the increased drain leakage current density after SiN_x deposition is undesired, it does not severely reduce the drain current swing. However, the increased gate leakage current significantly reduces the maximum breakdown voltage and hence the drain-source voltage swing, which obviously is detrimental for high-power device operation.

In this paper we present the RF power performance of AlGaN/GaN HEMTs with total gate widths (W_g) ranging from 80 μm up to 1 mm, which have been grown by metal-organic chemical vapour deposition (MOVPE) on 2 inch semi-insulating (s.i.) 4H-silicon carbide (4H-SiC) substrates. These devices have been fabricated using an optimized process flow comprising a low-power reactive ion etch (RIE) employing an argon (Ar) plasma after ohmic contact metallization [5], cleaning of the AlGaN surface prior to the Schottky gate metallization using a diluted ammonia (NH_4OH) solution [5], and passivation of the AlGaN surface using a PECVD SiN_x layer [6]. We will show that this process flow enables the fabrication of so-called dispersion-free AlGaN/GaN HEMTs and that devices with iron-doped GaN buffer layers (GaN:Fe) yield the highest RF output power.

Experimental and Discussion

Small-periphery devices

Devices with the following device dimensions: gate length (L_g) of 0.25 μm, W_g = 80 μm, unit gate width (W_{gu}) of 40 μm, gate-to-gate pitch (L_{gg}) of 60 μm, gate-source distance (L_{gs}) of 1 μm, gate-drain distance (L_{gd}) of 2 μm, and drain-source distance (L_{ds}) of 3.25 μm, which in this work are indicated as small-periphery devices, have been fabricated using the following process flow:

- BHF cleaning and rinse.
- Mesa etch: inductively-coupled plasma (ICP) process using Cl_2:H_2 chemistry.
- Ohmic contact metallization: Ti/Al/Ni/Au = 30/180/40/100nm.
- Dispersion treatment: RIE with Ar-plasma, 30W, 40mTorr, 30sec.
- Rapid thermal annealing of ohmic contacts: 800ºC, 2 min in N_2-ambient.
- Surface passivation: ammonia dip and deposition of 100 nm SiN_x.
- E-beam lithography for foot of gate and metallization: Ni/Au 20/40 nm
- E-beam lithography for top of gate and metallization: Ti/Au 20/380 nm

For the sub-micrometer gate contacts we have used so-called T-gates. The top of these gates is 0.75 μm wide and the extensions towards the source and drain contacts are both 0.25 μm long. The devices have been fabricated on 1x1 cm^2 samples from wafers indicated by the labels 1200, 1201, and 1203. The details of the corresponding structures and material properties are described in Table I. As can be observed from Table 1, all epitaxial structures contain 30nm undoped $Al_{0.26}Ga_{0.74}N$ barrier layers. Structure 1200 employs a very thin (1-2nm) additional aluminum nitride (AlN) layer between the AlGaN barrier and GaN buffer layer in order to improve the 2DEG sheet carrier density (n_s) resulting from better carrier confinement due to the larger potential step in the conduction band, and to improve the 2DEG mobility (μ) due to reduced alloy scattering at the AlN/GaN interface compared to the AlGaN/GaN interface. Structure 1201 acts as a reference. Structure 1203 consists of an iron-doped GaN buffer layer (GaN:Fe) in order to improve its semi-insulating properties and thereby reducing the drain leakage current.

Table I. Overview of the n.i.d. AlGaN/GaN epilayers on 2 inch s.i. 4H-SiC substrates.

Wafer	**Layer stack**	**d_{GaN} (µm)**	**d_{AlGaN} (nm)**	**Al (%)**	**R_{sheet} (Ωsq)**	**n_s (cm^{-2})**	**µ(cm^2/Vs)**
1200	AlGaN/AlN/GaN	1.2	30	26	350	9.5×10^{12}	1875
1201	AlGaN/GaN	1.2	30	26	440	9.3×10^{12}	1515
1203	AlGaN/GaN:Fe	1.4	30	26	530	8.8×10^{12}	1352

Figure 1 shows continuous wave (CW) DC current-voltage (I-V) measurement results for the processed small-periphery HEMTs. The output characteristics (I_D−V_{GS}) show maximum drain current densities at V_{GS} = +2 V of 1.2 A/mm, 1.1 A/mm, and 1.0 A/mm for structures 1200, 1201, and 1203, respectively. These current densities are in perfect agreement with the values that can be calculated using the material properties listed in Table I. In addition, it can be concluded that the very thin (1 - 2 nm) AlN layer between the AlGaN barrier and GaN buffer layers in structure 1200 indeed enhances both the density and mobility of the 2DEG electrons as this structure shows the highest drain current density. Furthermore, Fig. 1 shows that these structures have knee voltages (V_{knee}) as low as 4 V, which is excellent for achieving a large drain-source voltage swing provided that the breakdown voltage is high.

A serious drawback of these devices is the fact that the gate and drain leakage current densities ($I_{G,leak}$ and $I_{D,leak}$) at V_{DS} = 26 V and V_{GS} = -6 V are very high. The value of $I_{G,leak}$ is 11 mA/mm for all structures, and the values of $I_{D,leak}$ are 120 mA/mm, 100 mA/mm, and 80 mA/mm for structures 1200, 1201, and 1203 respectively. It has to be noted that structure 1203, whose GaN buffer layer has been intentionally doped with iron (Fe), shows the smallest drain leakage current. Although the large drain leakage currents reduce the drain current swing, the RF output power of these devices will be limited mostly by the breakdown voltage, which is strongly reduced because of the huge leakage currents of the 0.25 µm Schottky gates.

The off-state breakdown voltages of the devices on all structures were approximately as low as 35 V. From the transfer characteristics (I_D−V_{GS}) it can be seen that the devices on all structures are pinched-off at gate-source voltages (V_{GS}) of -6 V, and that the values of the maximum transconductance (g_m) are 220 mS/mm, 195 mS/mm, and 175 mS/mm for structures 1200, 1201, and 1203, respectively. Small-signal S-parameter measurements have been performed between 8 GHz and 12 GHz to determine values for the complex conjugated value of the measured output reflection coefficient (S^*_{22}), which can be used as a starting value for the load reflection coefficient (Γ_L) in the active load-pull measurements at 10 GHz.

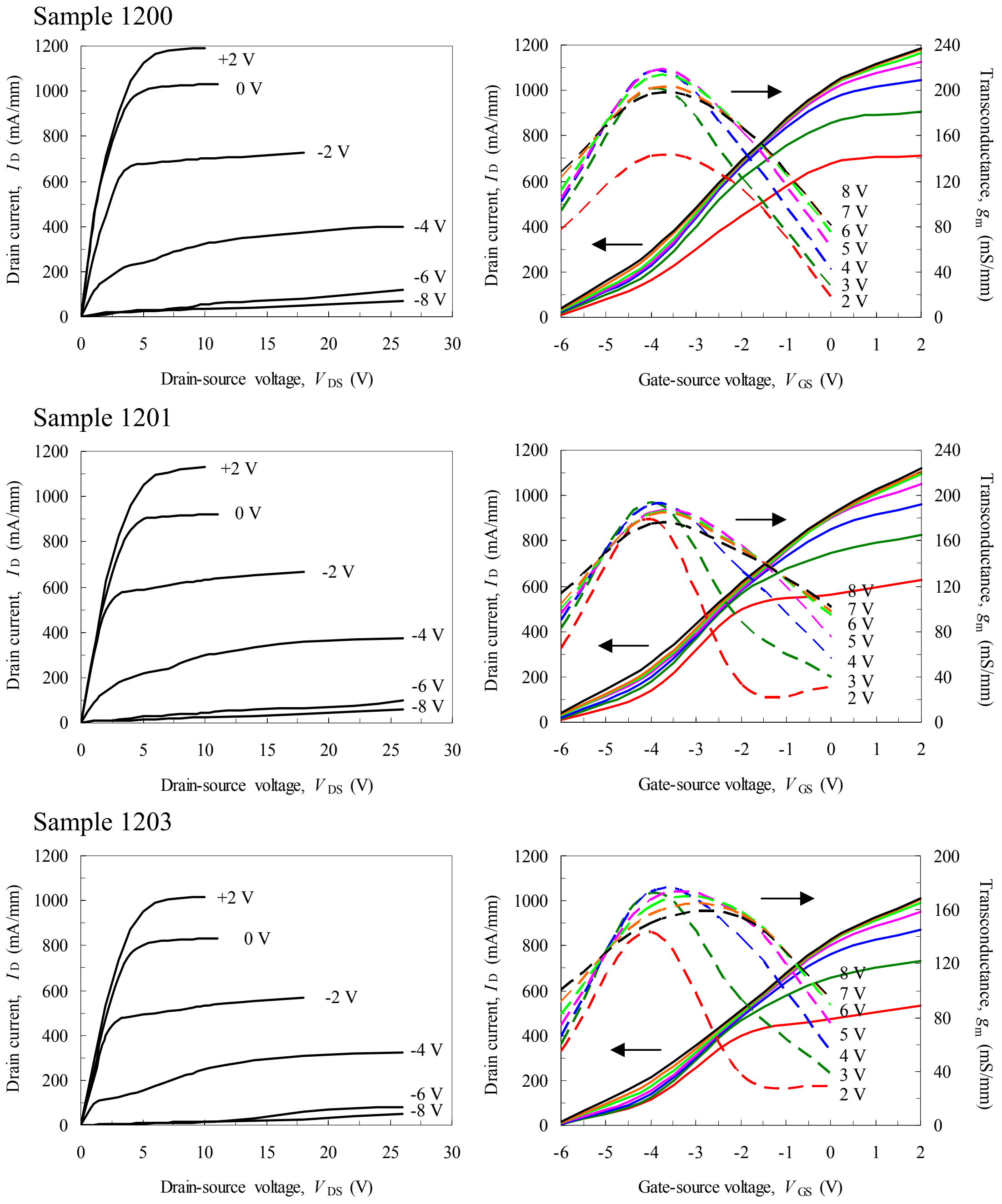

Figure 1. Continuous wave (CW) DC I-V measurement results of small-periphery (W_g = 80 µm) AlGaN/GaN HEMTs with sub-micrometer T-gates (L_g = 0.25 µm) on structures 1200, 1201, and 1203 respectively. The maximum DC power dissipated (P_{DC}) has been limited to 10 W.

Figure 2 shows the extrapolation of the values for the unity current-gain cut-off frequency (f_T) and maximum oscillation frequency (f_{max}) from the magnitudes in decibels of the current gain and the unilateral power gain, $|h_{12}|^2$ and |U| respectively, versus frequency. It can be seen that the values for f_T and f_{max} are 35 GHz and 75 GHz, respectively.

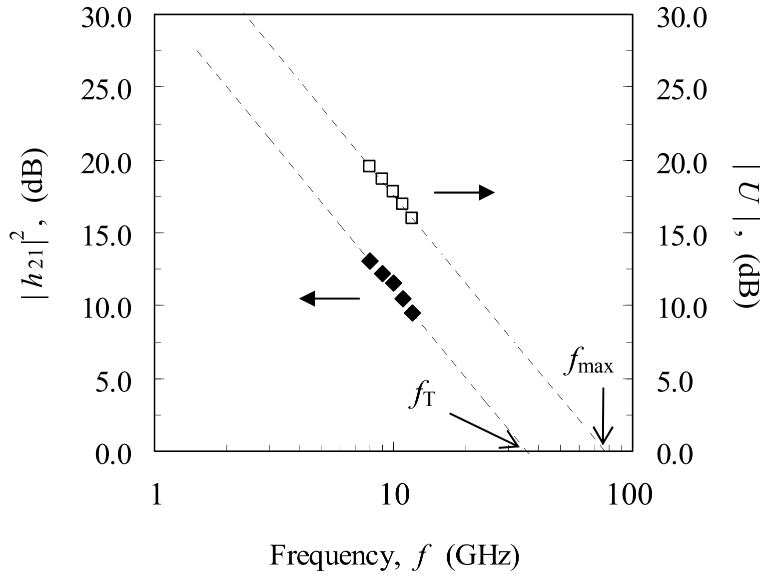

Figure 2. Extrapolation of the values for f_T and f_{max} for small (W_g = 80 μm) AlGaN/GaN HEMTs with sub-micrometer T-gates (L_g = 0.25 μm) on structures 1200, 1201, and 1203 respectively. The small-signal S-parameter measurements have been performed between 8 GHz and 12 GHz at V_{DS} = 26 V and V_{GS} = -3.5 V.

Pulsed DC I-V measurements showed that gate lag has successfully been eliminated for all devices on structures 1200, 1201, and 1203. This has been confirmed by CW active load-pull measurements using low drain-source bias voltages and small input powers (P_{in}). Single tone CW active load-pull measurements of a device on structure 1203, at 10 GHz with V_{DS} = 10 V, V_{GS} = -4 V, and $\Gamma_L = 0.7 + j\,0.45$, shows a maximum output power (P_{out}) of 17.4 dBm corresponding to 55.2 mW. Using the DC output characteristics of this structure, which are shown in Fig. 1(1203), we can calculate that the expected output power using the given bias conditions is (36.8 mA x 12 V) / 8 = 55.2 mW, exactly equals the measured output power at 10 GHz.

Finally, we have performed single tone CW active load-pull measurements at 10 GHz using class AB bias conditions (V_{DS} = 26 V and V_{GS} = -4 V) on all structures to determine values for the maximum output power density (P_D), associated power gain (G_p), and power added efficiency (PAE) of the small gate periphery AlGaN/GaN HEMTs. Values for P_D, G_P and PAE of 1.0 W/mm, 3.5 dB, and 4.3 %, respectively have obtained for structure 1200. For structure 1201 values for P_D, G_p, and PAE of 2.7 W/mm, 6 dB, and 13%, respectively have been obtained using the same load reflection coefficient as for structure 1200. Finally, for structure 1203 values for P_D, G_p, and PAE of 3.5 W/mm, 8 dB, and 26 %, respectively have been measured.

Considering the facts that the devices on all structures show dispersion free behavior at 10 GHz and have high maximum drain current densities of on average 1 A/mm, these load-pull results are very disappointing. The reason for these poor results obviously is the very low breakdown voltage caused by the excessively high gate and drain leakage currents. Comparison of the gate and drain leakage currents of the submicron T-gate devices and reference devices (L_g = 2 μm), processed at the same time, shows that the huge leakage currents are not introduced by the SiN_x deposition process as the 2-µm gate devices show values for $I_{G,leak}$ and $I_{D,leak}$ of 150 µA/mm and 400 µA/mm respectively.

The reason for the high leakage currents most likely is the use of titanium (Ti) in the top part of the T-gates. The T-gate consists of a Ni/Au = 20/40 nm foot and a Ti/Au = 20/380 nm top. Titanium has been chosen to achieve a good mechanical stability of the top part of the gates due to the good adhesion between Ti and the SiN_x passivation film. However, as the temperatures in the channel underneath the Schottky gates can get as high as 240 ºC [7], it is possible that Ti diffuses towards the AlGaN surface and lowers the Schottky barrier height. As a consequence, the gate leakage current increases and the breakdown voltage decreases. To circumvent this problem we have used Ni/Au for both the foot and top parts of the T- and field-plate (FP)-gates in the so-called large-periphery devices that will be described in the remainder of this paper.

Large-periphery devices

The so-called large-periphery devices have total gate widths (W_g) of 0.25 mm, 0.5 mm, and 1.0 mm, respectively. The unit gate widths (W_{gu}) of these devices are 62.5 µm, 100 µm, and 125 µm respectively. For the fabrication of the sub-micrometer gate contacts we have used T-gates and gates with a field-plate (FP) towards the drain contact. The gate length (L_g), which defines the footprint of the T- and FP-gates, has a constant value of 0.7 µm. The top of the T-gates is 1.2 µm wide with 0.25 µm extension towards the source and drain contacts. The remaining internal dimensions for all large periphery devices are: L_{gs} = 1.2 µm, L_{gd} = 3.0 µm, L_{ds} = 4.9 µm, and L_{gg} = 50 µm respectively. Air bridges are used to connect all individual drain contacts. The same holds for the individual source contacts. Devices have been designed using so-called comb- and fishbone-layouts.

All devices have been fabricated on 15 mm x 15 mm samples from structure 1203 because this structure showed the lowest gate and drain leakage currents. The following process flow has been used:

- BHF cleaning and rinse.
- Ohmic contact metallization: Ti/Al/Ni/Au = 30/180/40/100nm.
- Dispersion treatment: RIE with Ar-plasma, 30W, 40mTorr, 30sec.
- Rapid thermal annealing of ohmic contacts: 800ºC, 2 min in N_2-ambient.
- Mesa etch: inductively-coupled plasma (ICP) process using Cl_2:H_2 chemistry.
- Surface passivation: ammonia dip and deposition of 100 nm SiN_x.
- E-beam lithography for foot of gate foot and metallization: Ni/Au 20/150 nm
- E-beam lithography for top of gate and metallization: Ni/Au 20/250 nm
- Lithography for airbridges and RF contact pads followed by metallization of Ti/Au 20/1500 nm.

Note that the order of the mesa etch step and the ohmic contact formation has been changed and that the metallization of both the foot and top of the gate contacts has been changed.

Figure 3 shows CW DC I-V results for 0.25 mm, and pulsed DC I-V results for 0.5 mm and 1.0 mm T-gate devices. The output characteristics (I_D−V_{DS}) show drain current densities of 1.0 A/mm and 840 mA/mm at V_{GS} = +2 V and V_{GS} = 0 V respectively. These current densities are in perfect agreement with the values that can be calculated using the material properties listed in Table I and with the results for the small periphery devices. Figure 1 shows that the knee voltages (V_{knee}) for the output characteristics at V_{GS} = 0 V are 5 V. From the transfer characteristics (I_D−V_{GS}) it can be seen that all devices are pinched-off at VGS = -6 V, and that the values of the maximum g_m range from 180 mS/mm to 190 mS/mm.

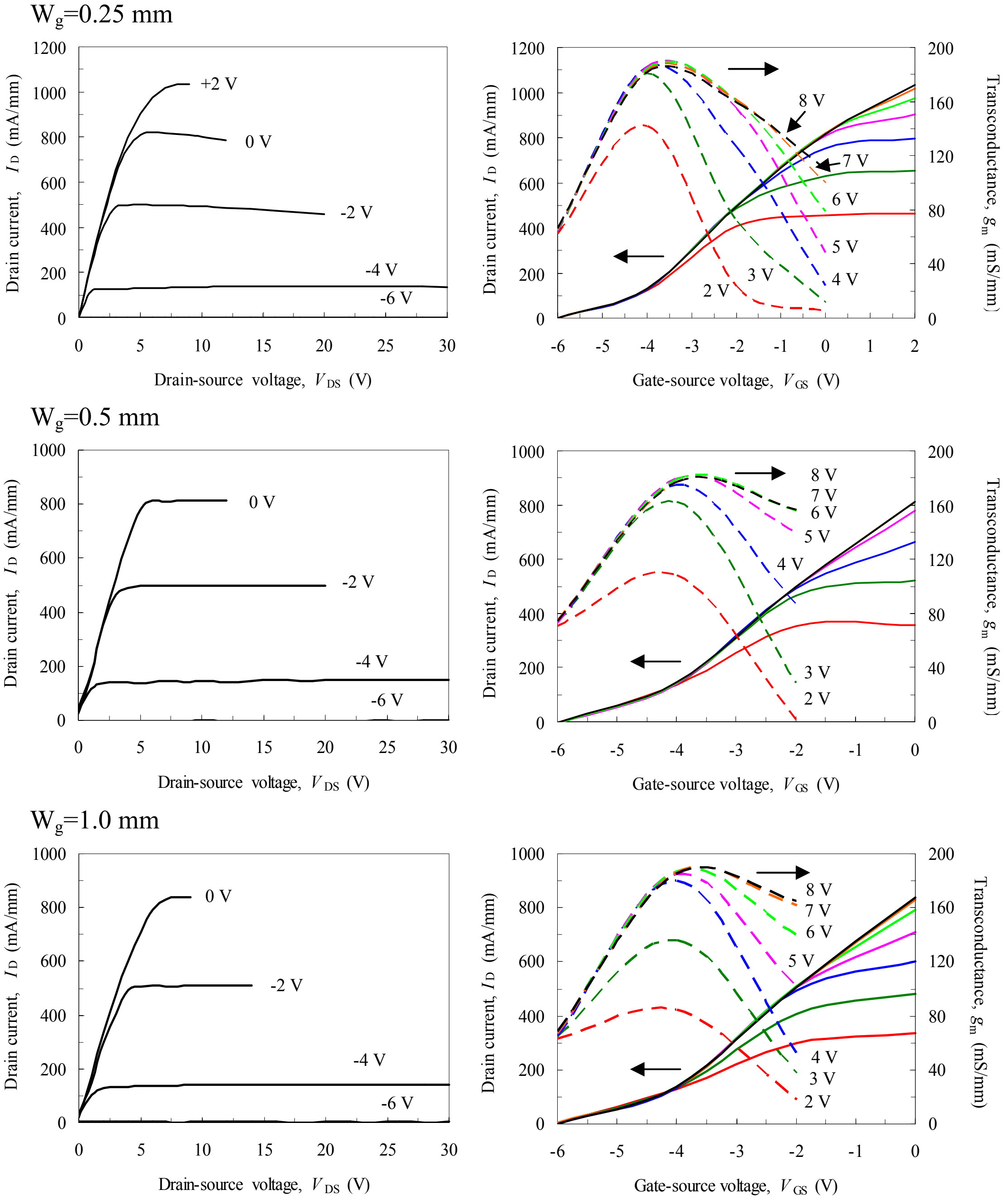

Figure 3. CW DC I-V results for 0.25 mm, and pulsed DC I-V results for 0.5 mm and 1.0 mm T-gate devices (L_g = 0.7 μm) with a comb layout on structure 1203. The maximum DC power dissipated (P_{DC}) has been limited to 10 W.

The off-state breakdown voltage ($V_{BD,off}$), which is defined as the drain-source voltage at which the gate leakage current reaches 1.0 mA/mm [8-9] for a completely pinched-off device, has been determined for a 1.0 mm T-gate HEMT with 10 gate fingers in a comb layout. Figure 4 shows that the device broke down at a drain-source voltage of 155 V, before the gate leakage current reached the 1.0 mA/mm level. This high breakdown voltage allows biasing of the devices at high drain-source voltages, e.g. V_{DS} = 60 V, to achieve a large voltage swing and a high RF output power. Furthermore, from Fig. 4 it has to be concluded that the implementation of the top parts of the T- and FP-gates with Ni/Au instead of Ti/Au has solved the problems of the large gate and drain leakage currents and the reduced breakdown voltage. For comparison with the small-periphery devices, the values of $I_{G,leak}$ and $I_{D,leak}$ at V_{DS} = 30 V and V_{GS} = -7 V are 200 μA/mm and 2 mA/mm, respectively.

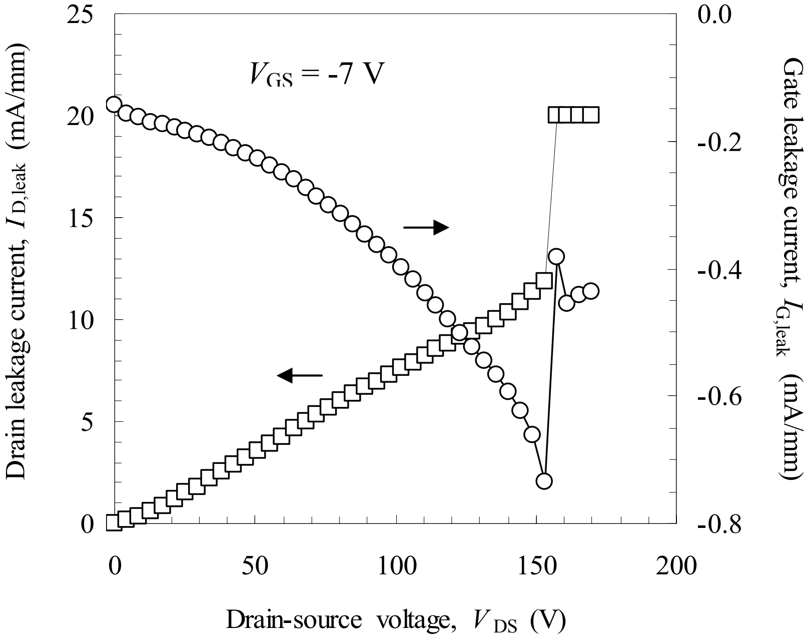

Figure 4. Measurement of the off-state breakdown voltage ($V_{BD,off}$) of a 1.0 mm T-gate HEMT with 10 gate fingers arranged in a comb layout at a gate-source voltage of -7 V.

Small-signal S-parameter measurements have been performed between 2 GHz and 4 GHz to determine values for S^*_{22}, which can be used as a starting value for Γ_L in the active load-pull measurements that have been performed at 2 GHz and 4 GHz, which are the lower and upper frequency limits, respectively of the so-called S-band. The values for f_T and f_{max} for a T-gate device in a comb layout with a total gate periphery of 0.25 mm are 12 and 34 GHz respectively.

Figure 5 shows active load-pull results for 0.25 mm (CW) (*left*), 0.5 mm (pulsed) (*middle*), and 1.0 mm (pulsed) (*right*) T-gate devices with a comb layout. The single tone measurements have been performed at 2 GHz under class AB bias conditions (V_{DS} = 50V, V_{GS} = -4.65V). It has to be noted that in the case of pulsed measurements the values for PAE could not be determined due to limitations of the measurement setup. Using Γ_L = 0.67 + j 0.21, values of 34.5 dBm (2.8 W), 15 dB, and 54 % have been measured for P_{out},

G_p, and PAE respectively of the 0.25 mm devices. For the 0.5 mm devices, P_{out} and G_p are 37.7 dBm (5.9 W) and 10.4 dB using $\Gamma_L = 0.35 + j\ 0.18$ and finally for the 1.0 mm devices P_{out} and G_p are 40.75 dBm (11.9 W) and 11 dB using $\Gamma_L = 0.06 + j\ 0.24$. From these results it has to be concluded that the maximum output power excellently scales as a function of W_g.

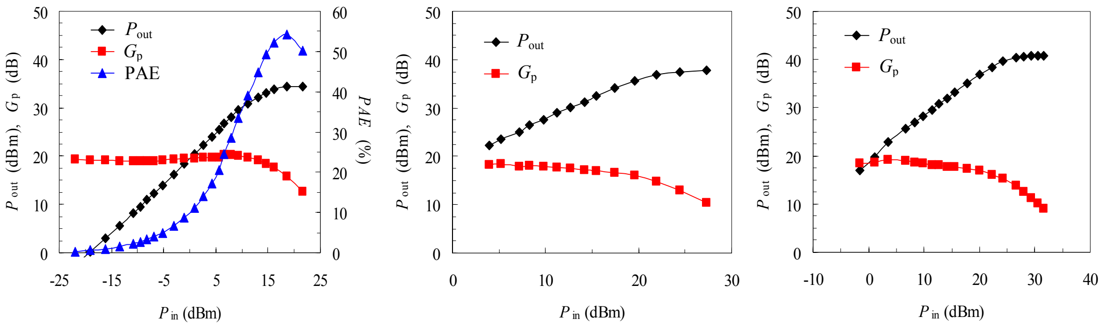

Figure 5. Single tone active load-pull results of 0.25 mm devices (*left*), 0.5 mm devices, pulsed (*middle*), and 1.0 mm devices, pulsed (*right*) at 2 GHz with $V_{DS} = 50$ V and $V_{GS} = -4.65$ V. All devices have T-gates arranged in a comb layout.

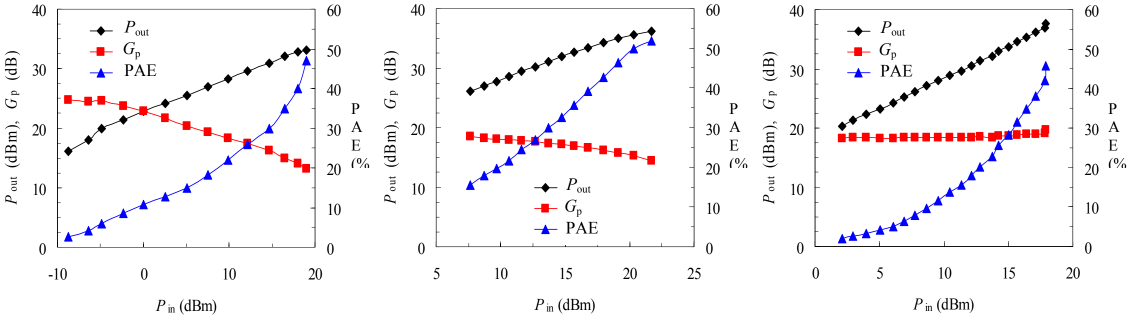

Figure 6. Single tone pulsed active load-pull results for 0.25 mm (*left*), 0.5 mm (*middle*) and 1.0 mm (*right*) T-gate devices with a comb layout at 4 GHz under class AB bias conditions ($V_{DS} = 40$ V, $V_{GS} = -4.0$ V).

Figure 6 shows single tone pulsed active load-pull results for 0.25 mm (*left*), 0.5 mm (*middle*), and 1.0 mm (*right*) T-gate devices with a comb layout at 4 GHz under class AB bias conditions ($V_{DS} = 40$ V, $V_{GS} = -4.0$ V). Using $\Gamma_L = 0.45 + j\ 0.45$, values of 33.1 dBm (2.05 W), 14 dB, and 47 % have been measured for P_{out}, G_p, and PAE of the 0.25 mm devices. For 0.5 mm devices, values of 36.1 dBm (4.07 W), 14.5 dB and 52 % have been obtained for P_{out}, G_p, and PAE using $\Gamma_L = 0.20 + j\ 0.50$. Finally, for the 1.0 mm devices values of 37.7 dBm (5.9 W), 19.8 dB, and 46 % have been achieved for P_{out}, G_p and PAE using $\Gamma_L = 0.10 + j\ 0.40$. It has to be noted that P_{out} of the 1.0 mm devices is less than can be expected from the scaling with W_g, which can clearly be observed for the 0.25 mm and 0.5 mm devices, because of the limited power available from the TWTA used. However, based on the scaling of P_{out} with W_g observed at 2 GHz and the scaling of the 0.25 mm and 0.5 mm devices at 4 GHz, it is reasonable to assume that the 1.0 mm devices can show an output power of 8 W at 4 GHz. It has to be noted that 0.25 mm devices with a FP-extension of 0.5µm towards the drain contact, i.e. their extension towards the drain is 0.25µm longer than the extension of the top of the T-gates, yield a maximum output power at 4 GHz under class AB conditions (V_{DS} = 60V, V_{GS} = -4.0V) of 2.95 W (11.8 W/mm), G_p = 14 dB, and PAE = 44%. This result is very similar to the maximum output power density achieved at 2 GHz.

Figure 7 provides a comparison of the maximum values of output power density (P_D) at S-band as a function of W_g of n.i.d. AlGaN/GaN HEMTs on s.i. SiC substrates that we have achieved in this work (diamonds) and that have been reported in literature (squares) [1,3,10-13]. It can be concluded that we have achieved state-of-the-art results with respect to the generation of large, i.e. 11.9 W, microwave output power for devices with large total gate widths, e.g. 1.0 mm.

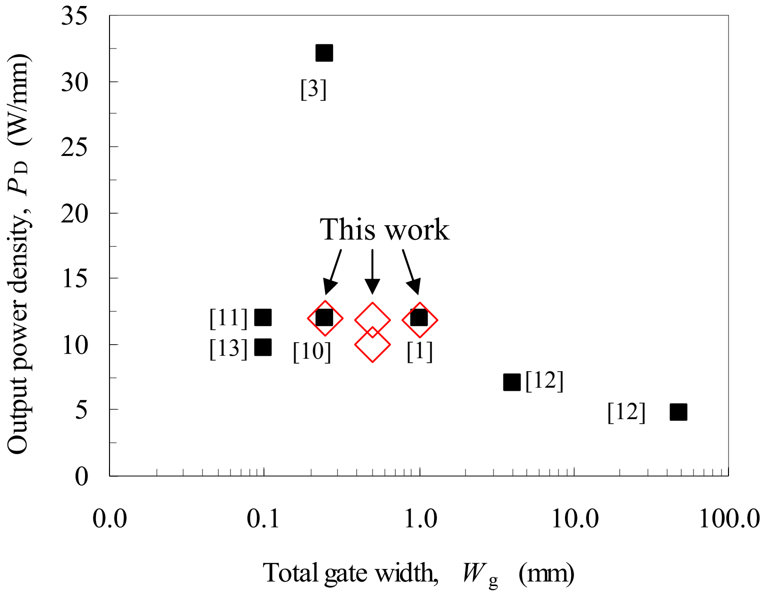

Figure 7. Comparison of P_D versus W_g for T-gate devices at 2 GHz and 4 GHz for V_{GS} = -4.65 V and V_{DS} is 30 V, 40 V, and 50 V, respectively.

Conclusions

We have demonstrated the successful fabrication of high-power, high-frequency large-periphery (W_g up to 1 mm) HEMTs using n.i.d. AlGaN/GaN:Fe epilayers grown by MOVPE on 2 inch s.i. SiC substrates. These dispersion-free devices are capable of yielding a maximum output power density of 11.9 W/mm at S-band (2-4 GHz) under class AB bias conditions (V_{DS} = 40 - 60 V, and V_{GS} = -4.65 – - 4.0 V). In order to achieve this result important processing improvements have been implemented like a high-quality SiN_x passivation layer, a low-power RIE Ar-plasma after ohmic contact metallization, a short dip in a diluted ammonia solution before the Schottky gate metallization, and replacing Ti by Ni in the top part of the T- or FP-gates with a constant L_g = 0.7 µm and values for W_g ranging from 0.25 mm - 1.0 mm. The gate and drain leakage currents at pinch-off are typically 200 µA/mm and 2 mA/mm, respectively. Moreover, excellent scaling of P_{out} with W_g has been demonstrated. In addition, the associated power gain ranges between 15 - 20 dB, and values for PAE varying from 54 - 70 % have been obtained.

References

1. Y. Ando, Y. Okamoto, K. Hataya, T. Nakayama, H. Miyamoto, T. Inoue, and M. Kuzuhara, “12 W/mm recessed-gate AlGaN/GaN heterojunction field-plate FET,” *Proc. IEEE International Electron Devices Meeting*. IEEE, p 563, 2003.
2. T. Kikkawa, T. Maniwa, H. Hayashi, M. Kanamura, S. Yokokawa, M. Nishi, N. Adachi, M. Yokoyama, Y. Tateno, and K. Joshin, “An over 200-w output power GaN HEMT push-pull amplifier with high reliability,” *IEEE MTT-S Digest*, p. 1347, 2004.
3. Y. F. Wu, A. Saxler, M. Moore, R. P. Smith, S. Sheppard, P. M. Chavarkar, T. Wisleder, U. K. Mishra, and P. Parikh, “30-W/mm GaN HEMTs by field plate optimizaztion,” *IEEE Electron Device Letters*, **25**, 117, 2004.
4. B. M. Green, K. K. Chu, E. M. Chumbes, J. A. Smart, J. R. Shealy, and L. F. Eastman, “The effect of surface passivation on the microwave characteristics of undoped AlGaN/GaN HEMTs”; *IEEE Electron Device* Letters; **21**; 268, 2000.
5. M.C.J.C.M. Krämer, R.C.P. Hoskens, B. Jacobs, J.J.M. Kwaspen, E.M. Suijker, A.P. de Hek, F. Karouta, and L.M.F. Kaufmann, “Dispersion free doped and undoped AlGaN/GaN HEMTs on sapphire and SiC substrates,” *Proc. Gallium Arsenide and other Compound Semiconductors Application Symposium 2004* (GAAS 2004), p75, 11 - 15 October 2004, Amsterdam, The Netherlands.
6. F. Karouta, M.C.J.C.M. Krämer, J.J.M. Kwaspen, A. Grzegorczyk, P. Hageman, B. Hoex, W.M.M. Kessels, J. Klootwijk, E. Timmering, and M.K. Smit, “Influence of the Structural and Compositional Properties of PECVD Silicon Nitride as a Passivation Layer for AlGaN HEMTs”, Paper#2079, 214th ECS meeting, 12-17 October, 2008, Honolulu, Hawaii.
7. J. C. Freeman, “Channel temperature model for microwave AlGaN/GaN HEMTs on SiC and sapphire MMICs in high power, high efficiency SSPAs”, NASA, Hanover, MD, 2004, TM-2004-212900.
8. Y. C. Chou, G. P. Li, Y. C. Chen, C. S.Wu, K. K. Yu, and T. A. Midford, “Off-state breakdown effects on gate leakage current in power pseudomorphic AlGaAs/InGaAs HEMT’s,” *IEEE Electron Device Letters*, **17**, 479, 1996.
9. M. H. Somerville, R. Blanchard, J. A. del Alamo, K. G. Duh, and P. C. Chao, “On-state breakdown in power HEMT’s: measurements and modeling,” *IEEE Transactions on Electron Devices*, **46**, 1087, 1999.
10. W. L. Pribble, J. W. Palmour, S. T. Sheppard, R. P. Smith, S. T. Allen, T. J. Smith, Z. Ring, J. J. Sumakeris, A.W. Saxler, and J.W. Milligan, “Applications of SiC MESFETs and GaN HEMTs in power amplifier design,” *IEEE MTT-S Digest*, 1819, 2002.
11. J. W. Johnson, E. L. Piner, A. Vescan, R. Therrien, P. Rajagopal, J. C. Roberts, J. D. Brown, S. Singhal, and K. J. Linthicum, “12 W/mm AlGaN-GaN HFETs on silicon substrates,” *IEEE Electron Device Letters*, **25**, 459, 2004.
12. Y. Okamoto, Y. Ando, K. Hataya, T. Nakayama, H. Miyamoto, T. Inoue, M. Senda, K. Hirata, M. Kosaki, N. Shibata, and M. Kuzuhara, “Improved power performance for a recessed-gate AlGaN-GaN heterojunction FET with a field-modulating plate,” *IEEE Transactions on Microwave Theory and Techniques*, **52**, 2536, 2004.
13. V. Desmaris, “Processing, characterization and modeling of AlGaN/GaN HEMTs”. Ph.D thesis, Chalmers University of Technology, ISBN 91-7291-734-2, 2006.